Effect of the chromophore donor group and ferrocene doping on the dynamic range, gain, and phase shift in photorefractive polymers

Eric Hendrickx, David Van Steenwinckel, and André Persoons
Laboratory of Chemical and Biological Dynamics, Center for Research on Molecular Electronics and Photonics, University of Leuven, Celestijnenlaan 200D, B-3001 Heverlee, Belgium

Celest Samyn
Laboratory of Macromolecular and Physical Organic Chemistry, University of Leuven, Celestijnenlaan 200F, B-3001 Heverlee, Belgium

David Beljonne
Chemistry of Novel Materials, Center for Research on Molecular Electronics and Photonics, University of Mons-Hainaut, Place du Parc 20, B-7000 Mons, Belgium

Jean-Luc Brédas
Chemistry of Novel Materials, Center for Research on Molecular Electronics and Photonics, University of Mons-Hainaut, Place du Parc 20, B-7000 Mons, Belgium and Department of Chemistry, The University of Arizona, Tucson, Arizona 85721-0041

(Received 6 April 2000; accepted 3 July 2000)

We have studied the photorefractive performance of poly(N-vinylcarbazole)-based composites doped with various concentrations of two structurally related dipolar chromophores, at 780 nm. The two chromophores had different electron donor groups, N,N-diethylamine and julolidine, respectively. Complete internal diffraction and gain coefficients >130 cm^{-1} were obtained for polymers doped with these chromophores. The polymers prepared with the chromophore having the strongest electron donor group, the julolidine group, had the largest dynamic range, but proved to be slower and had a smaller photorefractive phase shift. © *2000 American Institute of Physics.* [S0021-9606(00)70137-1]

I. INTRODUCTION

The photorefractive (PR) effect in electro-optic materials has been described as a refractive index modulation that is induced by a space-charge field. Because of their potential applications in the field of real-time holography, the search for robust and reliable PR materials has attracted much attention the past decades.[1] While the PR effect was observed first in inorganic crystals, recent research has demonstrated an efficient PR effect in organic materials, such as liquid crystals,[2] organic glasses,[3] and organic polymers.[4] Organic polymers combine the photorefractive advantages of high gain, resolution, and diffraction efficiency with the inherent low-cost processability and synthetic flexibility of polymers.

The components of an organic PR polymer composite reflect the subsequent steps that are necessary to produce the index modulation grating.[5,6] The polymer matrix is a photoconductor, frequently poly(N-vinylcarbazole) (PVK), that can be sensitized with a small amount of electron acceptor, such as (2,4,7-trinitro-9-fluorenylidene)malononitrile (TNFM). The charge-transfer complex formed between carbazole and TNFM has useful absorption in the infrared, and upon optical excitation and application of an electric field an electron is transferred from carbazole to TNFM. The hole is then free to migrate by hopping between adjacent carbazole units. The space-charge field established by the subsequent redistribution of charges reorients the polar dopant dyes in the polymer matrix, and the periodic orientation of the optically anisotropic dyes translates into a refractive index grating. A plasticizer, N-ethylcarbazole (ECZ), is added to lower the polymer glass transition temperature T_g to near room temperature and provides the necessary free volume to enable chromophore reorientation.

Thus far, a variety of chromophores has been tested as dopants in a carbazole matrix. The Bond Order Alternation theory has provided useful guidelines for the improvement of the PR chromophore figure-of-merit, and high diffraction efficiencies and gain coefficients in the infrared have been reported for highly polar chromophores with reduced aromaticity.[7] Another issue that has attracted attention recently is the effect of the chromophore's ionization potential (I_p). Chromophores with an I_p smaller than that of carbazole can act as compensating trap, and thereby reduce the PR grating phase and gain.[8] PR polymers having chromophores with high I_p also had faster grating buildup times.[9–11] Malliaras *et al.* have measured the photorefractive phase shift in polymers where the transport matrix contained different amounts of carbazole and another hole transport molecule (4-(diethylamino)benzaldehyde diphenylhydrazone) with smaller I_p. Doping the carbazole matrix with a small amount of the low I_p transport molecule resulted in a decrease of the photorefractive phase shift.[12] Thus, theoretically, an increase in the chromophore donor strength can increase the PR figure-of-merit, and improve the diffraction efficiency of the PR polymer, but will also reduce the chromophore I_p and thus lead to larger response times and smaller phase shifts and gain coefficients.

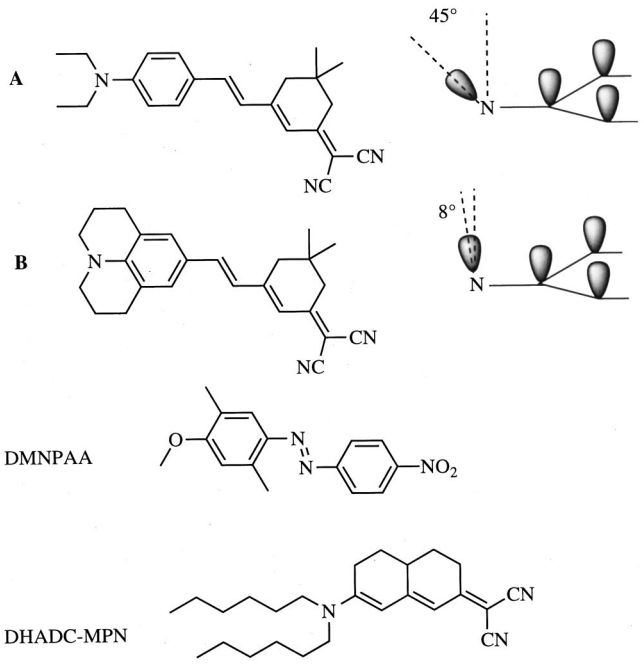

FIG. 1. Structure of the two chromophores used and the conformation of the donor group according to geometry optimizations with the Universal Force Field method. Structures of the chromophores DMNPAA and DHADC-MPN.

To investigate this possible trade-off, we have studied the two structurally related dyes shown in Fig. 1. Both dyes were doped at various concentrations into a PVK/ECZ matrix sensitized with 0.8 wt.% of TNFM. Complete internal diffraction and gain coefficients >130 cm^{-1} were observed at an excitation wavelength of 780 nm. We show that the small modification performed on the amino donor of the dye substantially affects the chromophore I_p and the PR figure-of-merit. The properties of the dyes and the complexation with TNFM are summarized in Sec. II. In Sec. III we analyze the evolution of the polymer photoconductivity and in Sec. IV the PR characterization with four-wave mixing and two-beam coupling is discussed. We have observed that composites doped with the chromophore with the strongest electron donor have the lowest I_p and the largest dynamic range, but also the slowest grating buildup speed and the smallest gain coefficient.

II. CHROMOPHORE PARAMETERS AND COMPLEXATION

The structures of the two dyes are shown in Fig. 1. Both chromophores are of the donor-π-acceptor type, with a dicyanovinyl acceptor, a conjugated system and an amino donor group. As has been demonstrated in studies on the first hyperpolarizability of organic chromophores, the incorporation of the amino donor into the julolidine group of chromophore **B** affects the conformation of the donor group and consequently the overlap of the nitrogen donor orbital with the conjugated system, and the donor strength.[13] In chromophore **B**, the *p* orbital of the amino donor is forced more into conjugation with the π-system of the phenyl ring. Geometries optimized at the molecular mechanics level with the universal force field (UFF) imply that the *p* orbital of the amino nitrogen makes an angle of 45° with the plane of the conjugated bridge in **A**, while in **B** this angle is 82° (the nitrogen atom has sp^2 hybridization).

TABLE I. Experimental and theoretical values for the dipole moment, ionization potential, position of the low-energy absorption maximum, and calculated values for the linear polarizability. The components of the linear polarizability tensor are calculated at 780 nm, and $\Delta\alpha=\alpha_{xx}-(\alpha_{yy}+\alpha_{zz})/2$.

	Chromophore **A**	Chromophore **B**
Dipole moment (exp, 1,4-dioxane)	9.3 D	11 D
Dipole moment (th, vacuum)	8.8 D	9.2 D
Ionization potential (exp, CH_2Cl_2)	5.40 eV	5.32 eV
Ionization potential (th, vacuum)	7.52 eV	7.33 eV
λ_{max} (exp, CH_2Cl_2)	499 nm	551 nm
α_{xx} (th)	56×10^{-24} esu	60×10^{-24} esu
α_{yy} (th)	28×10^{-24} esu	27×10^{-24} esu
α_{zz} (th)	4.0×10^{-24} esu	3.6×10^{-24} esu
$\Delta\alpha$ (th)	41×10^{-24} esu	45×10^{-24} esu
$\mu^2\Delta\alpha$ (th)	3.1×10^{-57} esu	3.8×10^{-57} esu

The experimental and theoretical data on chromophores **A** and **B** are summarized in Table I. The better overlap in **B** leads to a larger donor strength and ground-state dipole moment, in agreement with the larger experimental and theoretical dipole moment for **B**. The ionization potential I_p of the chromophore is determined by the energy of the HOMO orbital, that has a large weight on the amino donor. In chromophore **A**, the nitrogen donor orbital has a larger sp^3 character than in chromophore **B**. The lower conjugation in **A** leads to a larger I_p for chromophore **A**. The absorption maximum of the charge-transfer transition is red-shifted by 50 nm when going from chromophore **A** to chromophore **B**. The difference between the experimental and theoretical (gas-phase) dipole moment and I_p can be rationalized in terms of the Onsager reaction field stabilization of the ground-state charge separation[14] and the stabilization of the ions generated in the oxidation by solvation,[15] respectively.

The Gibbs function of solvation ΔG_s can be estimated from the Born equation.[15] This equation identifies ΔG_s with the electrical work of transferring an ion from vacuum into the solvent that is treated as continuous dielectric of relative permittivity ε_r:

$$\Delta G_s=\frac{z_i^2e^2N_A}{8\pi\epsilon_0 r_i}\left(1-\frac{1}{\varepsilon_r}\right), \tag{1}$$

where z_I is the charge on the ion, *e* the elementary charge, N_A Avogadro's number and r_i the radius of the ion. It can easily be verified that this equation predicts ΔG_s to be of the order 1.5 eV for a singly charged cation of radius 5×10^{-10} m in a medium of dielectric constant 10. This value is close to the difference between the ionization potential values from the calculations in vacuum and the cyclic voltammetry experiments in dichloromethane. In the Born equation, the molecular parameter that affects the Gibbs function of solvation is the ion size r_i. Both chromophores **A** and **B** have the same structure and similar substituents on the nitrogen donor atom, thus the r_i values for the two chromophores should also be similar. Using r_i values of 4.8×10^{-10} m and

4.7×10^{-10} m for chromophores **A** and **B**, respectively (calculated from the molar volume), the Born equation predicts a difference in solvation free energies of the order 0.03 eV, smaller than the 0.08 eV I_p difference in the liquid phase. Thus due to the similarity in chromophore structure, solvation or the polarity of the matrix does not affect the relative order of the ionization potentials and the relative position of the I_p values is expected to be similar in vacuum, polar solvents as dichloromethane, or the PVK matrix.

For the components of the linear polarizability tensor listed in Table I, the *x*-axis is defined in the direction of the dipole moment. The *y*-axis is in the plane of conjugation and perpendicular to the *x*-axis. The ground-state α_{xx} tensor component is larger for chromophore **B** than for chromophore **A**, leading to a larger linear polarizability anisotropy $\Delta\alpha$. Note that for both chromophores, the linear polarizability tensor has two large tensor components, α_{xx} and α_{yy}. The α_{zz} tensor component is small.

The calculated polarizability anisotropy $\Delta\alpha$ of chromophores **A** and **B** is similar to the experimental value of $\Delta\alpha$ reported for the azo compound 2,5-dimethyl-4-(p-nitrophenylazo)anisole (DMNPAA) at 690 nm (39×10^{-24} esu).[16] The orientational enhancement of the index modulation amplitude is proportional to $\mu^2\Delta\alpha$; due to their large dipole moments chromophores **A** and **B** have a $\mu^2\Delta\alpha$ value similar to that reported for 2-dihexylamino-7-dicyanomethylidene-3,4,4a,5,6-pentahydronaphthalene (DHADC-MPN, 9.8×10^{-57} esu at 690 nm, 5.7×10^{-57} esu at 830 nm), much larger than $\mu^2\Delta\alpha$ of DMNPAA (1.1×10^{-57} esu at 690 nm).[17] The structures of DMNPAA and DHADC-MPN are also shown in Fig. 1.

One approach to extend the sensitivity of the PR polymer to the working wavelength of 780 nm and to provide compatibility with low-cost laser diodes, is to add a small amount of an electron-deficient molecule, such as TNFM. TNFM forms a charge-transfer complex with carbazole that has useful absorption in the infrared, and upon excitation of the complex an electron is transferred from the carbazole unit to TNFM. As a complication, it has recently been shown that the dopant dyes can also complex with TNFM.[9] We have observed a complexation between chromophores **A** and **B**, and TNFM. The spectra of the chromophore-TNFM complexes in solution are shown in Fig. 2. Numerous studies on charge-transfer complexes have shown that, for a series of similar electron donors with an identical electron acceptor, the position of the charge-transfer absorption band correlates linearly with the donor I_p, shifting to longer wavelengths for smaller I_p values.[18] Since the I_p of the two dyes is much smaller than that of carbazole (I_p (carbazole)=5.9 eV),[19] the absorptivity of the chromophore-TNFM complex extends much farther into the infrared than for the TNFM-carbazole complex. The position of the complexation bands in Fig. 2 (**A**-TNFM: λ_{max}=830 nm; **B**-TNFM: λ_{max}=964 nm) agrees with the order of the I_p values.

We have measured the complexation constant and molar absorptivity at 780 nm of the complexes in acetone by analyzing the evolution of the optical density for a series of solutions with identical chromophore concentrations, but varying TNFM concentration. The analysis was done with

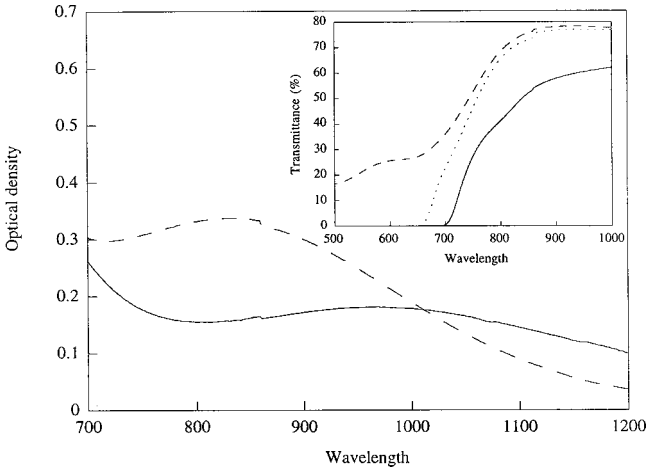

FIG. 2. Absorption spectra of the charge-transfer complexes formed between TNFM and chromophores **A** (dashed line, $[\mathbf{A}]=1.17\times10^{-3}$ M, [TNFM] = 0.0671 M) and **B** (full line, $[\mathbf{B}]=7.14\times10^{-4}$ M, [TNFM] =0.0335 M) in acetone. Inset: Transmittance of samples **B4** (full line), **BL** (dashed line) and **A4** (dotted line). See Table II for the polymer composition.

the Benesi–Hildenbrandt equation.[20] The stability constants and molar absorptivities at 780 nm for the chromophore **A**-TNFM and chromophore **B**-TNFM complexes were 5.6 M^{-1} (ε_{780}=970 $M^{-1}cm^{-1}$) and 7.3 M^{-1} (ε_{780}=1090 $M^{-1}cm^{-1}$), respectively. The higher stability constant for the chromophore **B**-TNFM complex is in line with the better electron-donating abilities of the julolidine nitrogen atom in chromophore **B**.

For ECZ-TNFM in acetone, a stability constant of 16 M^{-1} and ε_{780}=44 $M^{-1}cm^{-1}$ have been reported.[9] Thus, in a photorefractive polymer film both carbazole and chromophores will compete for complexation with TNFM. If the stability constant and extinction coefficients of the complexes in solution are extrapolated to the complexation in the polymer film, it can be expected, from the higher stability constant of the ECZ-TNFM complex and the larger carbazole concentration in the polymer, that the largest fraction of TNFM will be complexed with carbazole. However, due to their red-shifted absorption and much larger molar absorptivity at 780 nm, the small fraction of TNFM-chromophore complexes still reduces the transmittance at this wavelength.

III. PHOTOCONDUCTIVITY

To test the effect of the difference in chromophore structure on the optical properties, a series of polymers was prepared with increasing chromophore content. The polymer composition, numbering scheme, and extinction coefficients at 780 nm of the polymers are listed in Table II. In the concentration series, the PVK/ECZ ratio was varied slightly to keep the polymer T_g constant. The T_g of the polymers in Table II was measured by differential scanning calorimetry at a scanning rate of 20 °C/min and was found to lie in the range 17 ± 2 °C. The inset of Fig. 2 collects the absorption spectra of polymers **BL** (blank), **A4** and **B4**. In sample **BL**, no chromophore is present, and absorption in the 500–900 nm wavelength domain is due to the TNFM-carbazole complex. Doping this sample with either chromophore clearly

TABLE II. Numbering scheme, composition, and extinction coefficient of the polymers.

Sample	TNFM wt. %	ECZ wt. %	PVK wt. %	Chromophore wt. %	α (780 nm) cm^{-1}
BL	0.84	44	55	0	25
A1	0.83	43	55	**A** 0.83	29
A2	0.82	43	54	**A** 2.4	29
A3	0.82	40	54	**A** 4.9	30
A4	0.81	39	54	**A** 6.4	30
A5	0.82	37	52	**A** 10	42
A6	0.82	34	50	**A** 15	48
A7	0.98	27	45	**A** 27	63
B1	0.83	43	55	**B** 0.83	27
B2	0.82	43	54	**B** 2.5	55
B3	0.83	40	54	**B** 4.9	71
B4	0.81	39	54	**B** 6.4	77
B5	0.83	37	52	**B** 9.9	100
B6	0.83	35	49	**B** 15	130

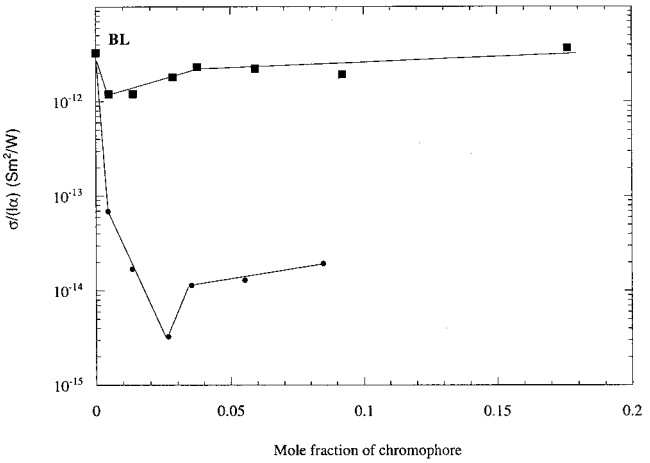

FIG. 3. Photoconductivity normalized by absorbed power for samples **BL**, **A1-7** (squares) and **B1-6** (circles). Conditions: Applied field $E=60$ V/μm, 150 ms light pulse, $\lambda=780$ nm, 7.2 mW optical power, area$=1.25\times10^{-5}$ m^2. The solid lines are guides to the eye.

results in a reduction of the transmittance. At the operating wavelength of 780 nm, doping with chromophore **B** results in a large decrease of the transmittance, while the effect of doping with a similar amount of chromophore **A** is smaller. Since chromophore **A** has a negligible molar absorptivity at 780 nm, the decrease in transmittance with increasing chromophore **A** loading can be attributed to the complexation between chromophore **A** and TNFM. Chromophore **B** has a red-shifted absorption spectrum compared to **A**, and a small molar absorptivity of 24 $M^{-1}\,cm^{-1}$ at 780 nm. Quantitatively, this molar absorptivity is insufficient to explain the decrease in transmittance at 780 nm with increasing chromophore **B** number density. Thus also in the materials based on chromophore **B**, a chromophore-TNFM complex is formed.

The production of a space-charge field in a photorefractive material involves the generation and migration of free charges. The efficiency of free charge generation is the photogeneration efficiency ϕ, defined as the number of free charges produced divided by the number of absorbed photons. The speed of the charge displacement in an externally applied electric field is quantified by the charge mobility, μ. A material parameter that is a convolution of the photogeneration efficiency and the charge mobility is the photoconductivity, σ_{ph}. The photoconductivity is related to the number density of free charges produced by light absorption n_D and the charge mobility by:[6]

$$\sigma_{ph}=n_D e\mu=\phi\frac{I\alpha}{h\nu}e\mu\tau, \tag{2}$$

where the charge number density has been written as a function of the photogeneration efficiency ϕ, the absorbed power $I\alpha$, the photon energy $h\nu$, and the charge carrier lifetime τ. e is the elementary charge.

Grunnet-Jepsen *et al.* have shown that by illumination of PVK/ECZ/chromophore/C_{60} mixtures for $\approx$10 min at 647 nm (optical irradiation 10 mW/cm^2) in an electric field of 20 V/μm, a fraction of C_{60} is photoreduced, and that the amount of C_{60}^- accumulated in the film scales with the chromophore I_p.[8] Simultaneously with the C_{60}^- buildup, a reduction in photoconductivity by a factor >10 and an increase in photorefractive grating buildup times have been observed, possibly caused by the trapping of charges by C_{60}^-.[8,9,11] We have tested if such a reduction in photoconductivity occurred in our PVK/ECZ/chromophore/TNFM mixtures at 780 nm with an electric field of 60 V/μm (optical irradiation 57.6 mW/cm^2); we have found that this occurs, but to a much lesser extent ($<50\%$ after 1 h of illumination in the aforementioned conditions). Thus the photoconductivity did not vary strongly during prolonged exposure, and the values reported here are for previously nonilluminated spots.

The evolution of the photoconductivity, normalized by absorbed power, with chromophore loading is shown in Fig. 3. From Eq. (2), this parameter is directly proportional to the product of photogeneration efficiency, charge carrier lifetime and mobility. Obviously, a large difference exists between the samples doped with chromophores **A** and **B**. Whereas doping PVK/ECZ (**BL**) with 0.83 wt. % of chromophore **A** (**A1**) only results in a threefold reduction in normalized photoconductivity, doping with 0.83 wt. % of chromophore **B** (**B1**) reduces the photoconductivity by a factor of over 40. The smallest normalized photoconductivity was observed for **B3**, 1000 times smaller than for **BL**. At higher chromophore doping levels, the photoconductivity in creases again, and for **A7** even surpasses that of **BL**.

The evolution of the normalized photoconductivity at low chromophore doping levels is similar to what was observed by Pai *et al.* for the mobility of PVK doped with small amounts of N,N′-bis(3-methylphenyl)-[1,1′-biphenyl]-4,4′-diamine (TPD).[21] Since the ionization potential of TPD is smaller than that of PVK, TPD in small concentrations acts as a trap for the holes that are being transported in the PVK-manifold and reduces the mobility by several orders of magnitude. Increasing the TPD concentration beyond 2 wt. % increases the probability of hole transport by hopping from TPD to TPD, and the mobility starts to increase again at a higher doping level.

As was the case for TPD in PVK, the I_p of the two

chromophores is smaller than that of carbazole. The I_p of chromophore **B** is smaller than that of chromophore **A**; accordingly we see the largest decrease in normalized photoconductivity for PVK/ECZ doped with chromophore **B**. For comparison, we have also measured the normalized photoconductivity of a PVK/ECZ/TNFM (**BL**) polymer doped with 1 wt.% of ferrocene. Ferrocene has an I_p of 5.19 eV ($E^0 = 0.69$ V vs SHE in CH_2Cl_2), even smaller than that of chromophores **A** and **B**. The doping with ferrocene in such small quantities did not affect the transmittance of the material at 780 nm, but resulted in a decrease of the normalized photoconductivity by a factor of 170, much larger than for doping with a similar amount of chromophores **A** and **B**. The evolution of the photoconductivity at low chromophore doping levels demonstrates that the chromophores at low concentrations act as a trap for hole-transport in the carbazole manifold.

Note that at higher chromophore concentrations the normalized photoconductivity increases again. For chromophore **B** at high concentrations we calculate that the largest fraction of the photons at 780 nm are absorbed by the TNFM-chromophore **B** complex. Also for the samples doped with a large amount of chromophore **A**, a large fraction of the absorbed photons produces a photoexcited chromophore **A**-TNFM complex. Dissociation of the optically excited complexes results in TNFM anions and chromophore **A**/**B** cations. The holes can then migrate by hopping from chromophore to chromophore, and the chromophore participates in the charge transport. Evidence of the charge-transporting capabilities of chromophore **A** was also provided by the good photorefractive properties of a polymer mixture of polycarbonate, chromophore **A** and TNFM. Due to the absence of a separate charge-transporter, such as carbazole, the photorefractive response can be explained by assuming that chromophores **A** participate to charge transport. In addition, the width of the density of states of the chromophore and carbazole hopping manifolds should increase due to the larger dipolar contribution to the energetic disorder.[22] While this effect is known to reduce the mobility, the increased concentration in chromophore hopping centers leads to the opposite effect (increasing the mobility). Thus at high doping levels, the density of states on average will be at lower energy and more broadened.

We have tested the effect on the photoconductivity of doping the materials with the highest chromophore concentrations, **A7** and **B6**, with 1 wt.% of ferrocene. The doping reduced the normalized photoconductivity by a factor of 3.3 and 3.7 for **A7** and **B6**, respectively. The decline of the normalized photoconductivity is smaller than for doping PVK/ECZ/TNFM (**BL**) with ferrocene and the reduction of the trapping potential of ferrocene can be seen as support for the thesis that the positive charges in chromophore doped polymers are being transported in a lower-lying manifold.

IV. PHOTOREFRACTIVE PROPERTIES

The diffraction efficiencies of the polymers in Table II were measured at 780 nm under steady-state conditions and the refractive index modulation amplitude was calculated using:[6]

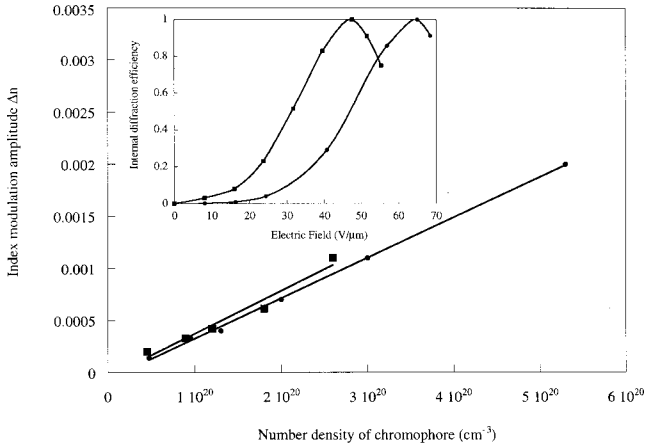

FIG. 4. Index modulation amplitude calculated from the diffraction efficiency at 50 V/μm of polymers **B2-6** (squares) and **A2-7** (circles) at 780 nm. Inset: Diffraction efficiency as a function of applied field for polymers **A7** (squares) and **B6** (circles). Even though chromophore **B** has the largest figure-of merit, the diffraction efficiency of **A7** is higher because of the larger chromophore **A** number density.

$$\Delta n = \frac{\arcsin\sqrt{\eta}}{564}. \tag{3}$$

564 is the numerical value of a combination of various constants, that depend on the geometry of the four-wave mixing experiments. The resulting plot of Δn as a function of chromophore number density at 50 V/μm is shown in Fig. 4. In agreement with the larger dipole moment and polarizability anisotropy of chromophore **B**, the **B** polymers have larger index modulation amplitudes at identical chromophore concentrations. For polymers **B6** and **A7** the evolution of the normalized diffraction efficiency with electric field is shown in the inset of Fig. 4.

Strutz and Hayden have demonstrated the possibility of writing photorefractive and photochemical gratings in a polymer composite of PVK/ECZ/C_{60}/chromophore **A** at 7 wt.% chromophore loading.[23] The photochemical grating was written at a wavelength of 675 nm and involved triplet–triplet energy exchange between the photoexcited C_{60} and chromophore **A**. We have used the sensitizer TNFM and a working wavelength of 780 nm, and have only observed reversible, field-dependent photorefractive gratings.

Harper *et al.* have shown that for highly polar anisotropic chromophores at high concentrations, chromophore–chromophore electrostatic interactions occur that counteract the alignment of the chromophores by an external field.[24] Due to these chromophore–chromophore interactions, the dependence of the electro-optic coefficient on chromophore number density is no longer linear, as predicted by the oriented gas model, but shows a maximum. If the oriented gas model is applied to low T_g polymers, the index modulation amplitude scales with the photorefractive chromophore number density N as:[6]

$$\Delta n = N(A\mu^2\Delta\alpha + B\mu\beta)E_{SC}E_{EXT}, \tag{4}$$

where various constants are combined in A and B, such as local field and geometry factors, and E_{SC} and E_{EXT} are the amplitudes of the space-charge field and applied field, re-

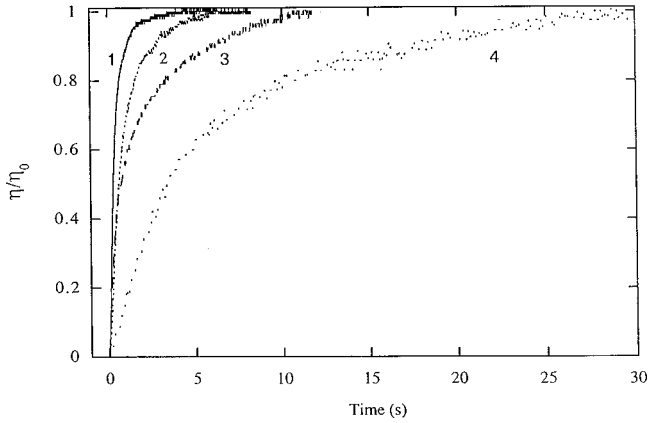

FIG. 5. Evolution of the normalized diffraction efficiency as a function of time for materials **A7** (1), **A7**+1 wt. % ferrocene (2), **B6** (3), and **B6** + 1 wt. % ferrocene (4). The sample was kept at an electric field of 48 V/μm with one writing beam on for 3 min. Then the second writing beam was turned on at $t=0$ s, and the build-up of the diffracted intensity was monitored.

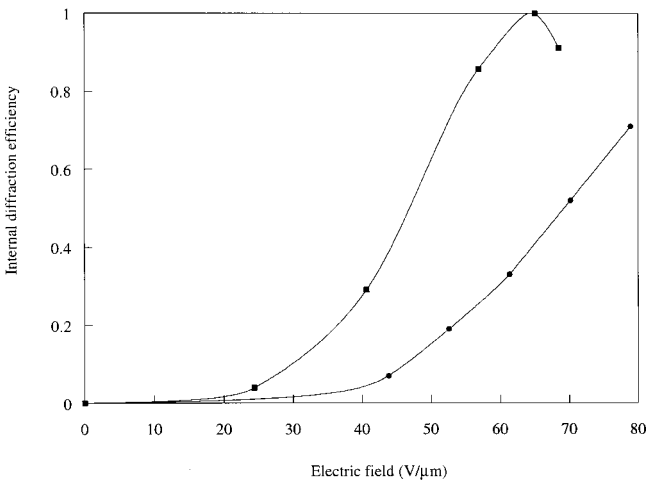

FIG. 6. Diffraction efficiency as a function of electric field for **B6** (squares) and **B6** doped with 1 wt. % of ferrocene (circles).

spectively. Whereas the linear relation between Δn and N is sometimes seen as evidence that chromophore–chromophore interactions can be neglected, it does not prove the absence of these interactions. Quantitatively, the Δn values calculated from the $\mu^2\Delta\alpha$ are larger than those observed experimentally, which can indicate aggregation.

Figure 5 shows the evolution of the normalized diffraction efficiency as a function of time for samples **B6**, **A7**, **B6** doped with 1 wt. % of ferrocene, and **A7** doped with 1 wt. % of ferrocene. The incorporation of the amino donor in a julolidine group improves the diffraction efficiency; however when comparing **A7** to **B6**, the speed of the grating build-up decreases strongly. The addition of 1 wt. % ferrocene to **A7** and **B6** results in a further increase of the grating buildup time.

Writing of a photorefractive grating in low-T_g polymers involves the steps of charge generation, charge migration, and chromophore reorientation. Since the PVK/ECZ ratio was varied to keep the T_g constant to within 4 °C and the chromophores have similar structures, the speed of reorientation should be similar for the materials in Fig. 5. The speed of the space-charge field build-up, however, depends on the processes of charge generation and migration, just as the photoconductivity. The parallel evolution of build-up time and photoconductivity, as discussed in Sec. III, shows that **B6** and the ferrocene doped polymers are slower due to the reduced speed of the space-charge field buildup. A correlation between photoconductivity and grating build-up time has also been reported in Refs. 9, 11, and 25. Zilker and co-workers have also shown that a more dispersive charge transport leads to a slower holographic response.[26]

The doping of **B6** with ferrocene also results in a decrease in steady-state amplitude of the diffracted beam. This evolution is shown in Fig. 6. Since doping with ferrocene does not affect the chromophore concentration or T_g, the achievable refractive index modulation by birefringence remains identical. As shown by the evolution of photoconductivity, the largest effect of ferrocene doping is on the space-charge field. The amplitude of the steady-state space-charge field is:[1]

$$E_{SC}^2=\left(\frac{\sigma_{ph}}{\sigma_{ph}+\sigma_{\text{dark}}}\right)^2\frac{E_D^2+E_{OG}^2}{(1+(E_D/E_q))^2+(E_{OG}/E_D)^2}, \tag{5}$$

where σ_{ph} and σ_{dark} are the photo and dark conductivities, $E_D=2\pi k_BT/e\Lambda$ the diffusion field, $E_q=N_T\Lambda e/2\pi\varepsilon_0\varepsilon_r$ the trap-limited field, and E_{OG} the component of the applied field along the grating vector; k_B is the Boltzmann constant, T the temperature, e the electron charge, Λ the grating period, and ε_0 and ε_r are the permittivity of vacuum and the static dielectric constant, respectively. The first ratio can be seen as the washing out of the space-charge field that takes place if the magnitude of the dark conductivity approaches that of the photoconductivity.

We have measured the photoconductivity and dark conductivity of **B6** and **B6** doped with ferrocene at an applied field of 60 V/μm. Due to the lowering in photoconductivity upon doping with ferrocene, the ratio $\sigma_{ph}/(\sigma_{ph}+\sigma_{\text{dark}})$ drops from 0.85 to 0.39, leading to a twofold decrease in the amplitude of the space-charge field according to Eq. (5). From Eq. (4), the refractive index modulation amplitude is directly proportional to the amplitude of the space-charge field, and will therefore also be reduced by a factor 2. From Eq. (3) and the data in Fig. 6, the index modulation amplitudes at 60 V/μm are calculated to be 1.1×10^{-3} and 1.9×10^{-3} for **B6** doped with ferrocene and **B6**, respectively.

The gain coefficients at an electric field of 50 V/μm as a function of chromophore concentration are shown in Fig. 7. Two tendencies can clearly be observed: the gain coefficient increases with chromophore concentration, and at identical concentrations the gain for materials **A2-7** is larger than or similar to the gains for **B4-6**, although the dynamic range was larger for the **B** samples. The gain coefficients of polymers **A7** and **B6** as a function of electric field are shown in the inset of Fig. 7.

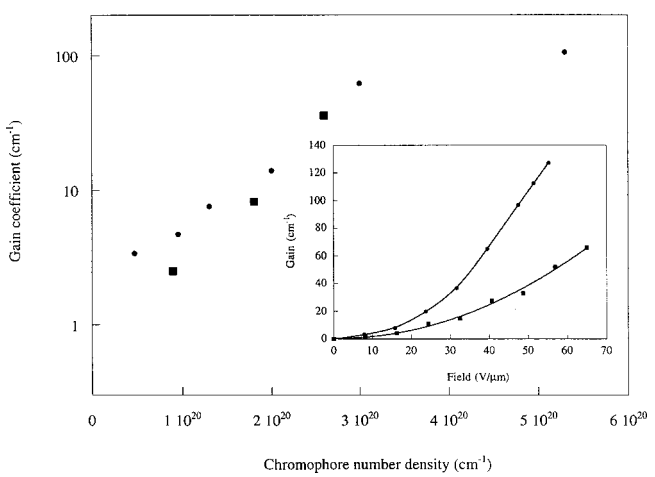

FIG. 7. Gain coefficient at an applied field of 50 V/μm as a function of chromophore number density for polymers doped with chromophore **A** (circles) and **B** (squares). Inset: Gain coefficient as a function of applied field for materials **A7** (circles) and **B6** (squares).

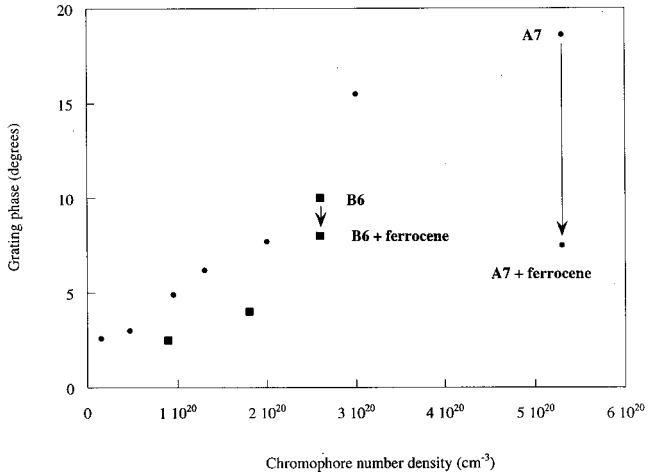

FIG. 8. Photorefractive phase shift calculated from gain coefficient and diffraction efficiency as a function of chromophore number density for polymers doped with chromophore **A** (circles) and **B** (squares). The field was 48 V/μm. The arrows show the change in phase shift found upon doping the polymers **A7** and **B6** with 1 wt. % of ferrocene.

The increase of the gain coefficient with chromophore concentration can partly be rationalized by the dependence of the gain coefficient on the refractive index modulation amplitude:

$$\Gamma = \frac{4\pi}{\lambda}(\bar{e}_1 . \bar{e}_2^*)\Delta n \sin\theta, \tag{6}$$

where λ is the optical wavelength, $\bar{e}_1$ and $\bar{e}_2$ are the polarization vectors of the two writing beams, and θ is the photorefractive phase shift between the space-charge field and the interference pattern generated by the interacting beams. From Eq. (6) and the index modulation amplitudes in Fig. 4, we have calculated the photorefractive phase shifts. The evolution of the phase shift with chromophore concentration is shown in Fig. 8. An increase in chromophore concentration produces a larger phase shift, and coincides with the increased photoconductivity at higher chromophore concentrations. The lower gain coefficient of the polymers doped with chromophore **B** is also explained by a smaller phase shift.

This evolution of the photorefractive phase shift with chromophore concentration and ionization potential is similar to what has been reported by Malliaras *et al.*[12] These authors have modified the composition of the photorefractive hole-transporting matrix by adding a transport molecule with low ionization potential, 4-(diethylamino)benzaldehyde diphenylhydrazone (DEH), to PVK. Doping a small amount (<5 wt. %) of DEH in the PVK matrix causes a strong decrease in phase shift. At higher concentrations, the phase shift increases again, due to the contribution of DEH to the hole transport. For our polymers with low chromophore concentration, the photorefractive phase shift was difficult to calculate due to the experimental errors on gain and diffraction efficiency. At higher chromophore concentrations, the increase in photoconductivity and phase shift with chromophore concentration suggests that the chromophore acts as a trap at low concentrations and starts to participate in charge-transport at high concentrations.

The smaller phase shift for composites based on chromophore **B** compared to chromophore **A** can be attributed to the smaller I_p or better trapping potential of chromophore **B**. In the model proposed by Grunnet-Jepsen *et al.*, a chromophore with small I_p acts as a better compensator and a larger concentration of photoreduced sensitizer will accumulate in the polymer. Since this photoreduced sensitizer acts as the photorefractive trap, a larger concentration of this trap produces a smaller photorefractive phase shift.[8] In Fig. 8, the arrows indicate the change in phase shift induced by doping materials **A7** and **B6** with small amounts of ferrocene. Clearly, adding 1 wt. % of ferrocene further reduces the phase shift, in agreement with the low I_p of ferrocene compared to the other components in the photorefractive mixture.

We have also reported on the phase shifts of two polymers doped with structurally related dyes with higher ionization potential than chromophore **A**.[10] These polymers, at similar doping levels, also exhibited a larger photorefractive phase shift than is observed in polymers with chromophores **A** and **B**.

V. CONCLUSION

In conclusion, we have prepared photorefractive polymers doped with different concentrations of two chromophores. These chromophores have identical conjugation paths and acceptor groups, but differ in the nature of the electron-donating groups: either diethylamine or julolidine moieties. Quantum-chemical calculations show that the julolidine group is the strongest electron donor, leading to a larger dipole moment and smaller ionization potential. Both chromophores form a charge-transfer complex with the sensitizer TNFM, which results in a larger absorptivity of the photorefractive polymers at the operating wavelength of 780 nm as the chromophore concentration increases.

At identical chromophore concentrations, the larger asymmetry induced by the julolidine group proves beneficial for obtaining a higher dynamic range. The dependency of the

dynamic range on the chromophore number density is found to be linear. The polymers based on the chromophore with the diethylamine donor, however, have a larger photorefractive phase shift and a smaller buildup time. The photorefractive phase shift increases with chromophore concentration. These tendencies can be understood by considering the possibility that a positive charge can be trapped and transported within the chromophore manifold. Photoconductivity experiments provide evidence for this scenario. As an other illustration of the effect of charge trapping on the phase shift and response time, samples doped with chromophore and a small amount of ferrocene have been tested. Addition of ferrocene results in a further increase in the response time and a decrease in photorefractive phase shift.

VI. EXPERIMENTAL/THEORETICAL APPROACH

For the quantumchemical calculations, the geometry optimizations have been performed at the molecular mechanics level, using the Universal Force Field (UFF),[27] and the excited states were calculated with the INDO[28]/SCI approach. The ionization potential was obtained by applying Koopman's Theorem at the INDO level. The linear polarizability tensor components are from fully converged Sum-Over-States calculations.

Chromophore **A** was purchased from Chromophore Inc.. Chromophore **B** was synthesized by reaction of 2-(3,5,5-trimethylcyclohex-2-ene-1-ylidene)-1,3-propanedinitrile and 4-formyljulolidine in dimethylformaldehyde solution in the presence of acetic acid, acetic anhydride, and pyridine.[29] The crude product was purified by column chromatography (silicagel/ethylacetate) and yielded dark blue crystals with m. p. 218.5–219.9 °C.

^{1}NMR ($CDCl_3$): $\delta=1.1$ (s; 6H), 1.6 (s; 4H), 2.0 (m, 4H), 2.78 (t, 4H), 3.29 (t, 4H), 6.77 (s, 1H), 6.79 (d, 1H), 7.0 (d, 1H); 7.3 (s, 2H).

Experimentally, the ground-state dipole moment was determined by analyzing the evolution of the dielectric constant of a dilution series of the chromophore in 1,4-dioxane according to the theory in Ref. 30. The experimental chromophore I_p was calculated from cyclic voltammetry experiments using the ferrocene/ferrocenium-ion couple ($E^0=0.69$ V) as internal standard:

$$I_{p,\mathrm{chrom}}(eV)=E^0(V)+4.5, \tag{7}$$

where $E^0(V)$ is the redox potential of the chromophore versus the standard hydrogen electrode. The redox potential was measured in dichloromethane with 0.1 M tetrabutylammonium hexafluorophosphate at a scanning speed of 250 mV/s using platina working and counter electrodes and a silver reference electrode. For both chromophore **A** and **B** the oxidation was reversible, and the redox potential was taken as the average of the anodic oxidation and reduction peaks.

We have measured the photoconductivity σ_{ph} by measuring the voltage change over a resistor ΔV (resistance $R=1$ MΩ) in series with a biased (applied field $E=60$ V/μm) sample when it was illuminated with a 150 ms light pulse ($\lambda=780$ nm, 7.2 mW optical power, area $S=1.25\times10^{-5}$ m^2):

$$\sigma_{ph}=\frac{\Delta V}{RES}. \tag{8}$$

The photorefractive characterization of the samples was performed by measuring steady-state diffraction efficiencies and two-beam coupling gain coefficients as a function of applied field. A degenerate four-wave mixing technique was used to obtain diffraction efficiencies.[4] The two writing beams were s-polarized, had a power of 2.8 mW each, and were collimated to 300 μm diameter inside the sample. The probe beam was *p*-polarized, collimated to a diameter of 150 μm and had a power of 2 μW. The normalized diffraction efficiency was calculated as the ratio of the intensity of the diffracted probe beam I_{diff} and the intensity of the transmitted probe I_t without the diffraction grating:

$$\eta=\frac{I_{\mathrm{diff}}}{I_t}. \tag{9}$$

In the two-beam coupling experiments, the photorefractive grating was written with two *p*-polarized writing beams. The gain coefficient Γ was calculated as:

$$\Gamma d=\cos\alpha_1\left(\ln\frac{I_1^t(I_2\neq0)}{I_1^t(I_2=0)}\right)-\cos\alpha_2\left(\ln\frac{I_2^t(I_1\neq0)}{I_2^t(I_1=0)}\right). \tag{10}$$

I_1^t and I_2^t are the transmitted intensities of writing beams 1 and 2, α_1 and α_2 are the angles between the writing beams and the normal to the sample, and d is the sample thickness.

ACKNOWLEDGMENTS

E.H. is a postdoctoral fellow and D.V.S. a research assistant of the Fund for Scientific Research-Flanders (Belgium) (FWO). D.B. is a research fellow of the Belgian National Fund for Scientific Research (FNRS). This research was supported by research grants from the FWO (G.0308.96, 1.5.009.99), the University of Leuven (GOA/95/01). The collaboration between the Universities of Leuven and Mons is conducted in the framework of the Belgian Federal Government Inter-University Attraction Pole–IUAP P4/11.

[1] *Photorefractive Materials and Their Applications*, edited by P. Günter and J. P. Huignard (Springer, Berlin, 1988, 1989), Vols. I and II.
[2] C. Khoo, H. Li, and Y. Liang, Opt. Lett. **19**, 1723 (1994).
[3] M. P. Lundquist, R. Wortmann, C. Geletneky, R. J. Twieg, M. Jurich, V. Y. Lee, C. R. Moylan, and D. M. Burland, Science **274**, 1182 (1996).
[4] K. Meerholz, B. L. Volodin, Sandalphon, B. Kippelen, and N. Peyghambarian, Nature (London) **371**, 497 (1994).
[5] W. E. Moerner and S. M. Silence, Chem. Rev. **94**, 127 (1994).
[6] B. Kippelen, K. Meerholz, and N. Peyghambarian, in *Nonlinear Optics of Organic Molecules and Polymers*, edited by H. S. Nalwa and S. Miyata (Chemical Rubber, Boca Raton, FL, 1997), p. 465.
[7] B. Kippelen, S. R. Marder, E. Hendrickx, J. L. Maldonado, G. Guillemet, B. L. Volodin, D. D. Steele, Y. Enami, Sandalphon, Y. J. Yao, J. F. Wang, H. Röckel, L. Erskine, and N. Peyghambarian, Science **279**, 54 (1998).
[8] A. Grunnet-Jepsen, D. Wright, B. Smith, M. S. Bratcher, M. S. DeClue, J. S. Siegel, and W. E. Moerner, Chem. Phys. Lett. **291**, 553 (1998).
[9] E. Hendrickx, Y. Zhang, K. B. Ferrio, J. A. Herlocker, J. Anderson, N. R. Armstrong, E. A. Mash, A. P. Persoons, N. Peyghambarian, and B. Kippelen, J. Mater. Chem. **9**, 2251 (1999).
[10] D. Van Steenwinckel, E. Hendrickx, K. Van Den Broeck, C. Samyn, and A. Persoons, J. Chem. Phys. **112**, 11030 (2000).
[11] M. A. Diaz-Garcia, D. Wright, J. D. Casperson, B. Smith, E. Glazer, W.

E. Moerner, L. I. Sukhomlinova, and R. J. Twieg, Chem. Mater. **11**, 1784 (1999).
[12] G. G. Malliaras, V. V. Krasnikov, H. J. Bolink, and H. Hadziiannou, Appl. Phys. Lett. **66**, 1038 (1995).
[13] M. Blanchard-Desce, V. Alain, P. V. Bedworth, S. R. Marder, A. Fort, C. Runser, M. Barzoukas, S. Lebus, and R. Wortmann, Chem. Eur. J. **3**, 1091 (1997).
[14] A. R. Blythe, *Electrical Properties of Polymers* (Cambridge University Press, Cambridge, 1979), p. 33.
[15] P. W. Atkins, *Physical Chemistry* (Oxford University Press, Oxford, 1990), p. 248.
[16] Sandalphon, B. Kippelen, K. Meerholz, and N. Peyghambarian, Appl. Opt. **35**, 2346 (1996).
[17] E. Hendrickx, B. D. Guenther, Y. Zhang, J. F. Wang, K. Staub, Q. Zhang, S. R. Marder, B. Kippelen, and N. Peyghambarian, Chem. Phys. **245**, 407 (1999).
[18] M. W. Hanna and J. L. Lippert, in *Molecular Complexes*, edited by R. Foster (Elek Science, London), p. 9.
[19] J. F. Ambrose and R. F. Nelson, J. Electrochem. Soc. **115**, 1159 (1968).
[20] R. Foster, in *Molecular Complexes*, edited by R. Foster (Elek Science, London), p. 124.
[21] D. M. Pai, J. F. Yanus, and M. Stolka, J. Phys. Chem. **88**, 4714 (1984).
[22] P. M. Borsenberger and D. S. Weiss, in *Organic Photoreceptors for Xerography* (Marcel Dekker, New York, 1998), p. 319.
[23] S. J. Strutz and L. M. Hayden, Appl. Phys. Lett. **74**, 2749 (1999).
[24] A. W. Harper, S. Sun, L. R. Dalton, S. M. Garner, A. Chen, S. Kalluri, W. H. Steier, and B. H. Robinson, J. Opt. Soc. Am. B **15**, 329 (1998).
[25] D. Wright, M. A. Diaz-Garcia, J. D. Casperson, M. DeClue, and R. J. Twieg, Appl. Phys. Lett. **73**, 1490 (1998).
[26] U. Hofmann, M. Grasruck, A. Leopold, A. Schreiber, S. Schloter, C. Hohle, P. Strohriegl, D. Haarer, and S. J. Zilker, J. Phys. Chem. B **104**, 3887 (2000).
[27] C. J. Casewit, K. S. Colwell, and A. K. Rappé, J. Am. Chem. Soc. **114**, 10046 (1992).
[28] J. E. Ridley and M. C. Zerner, Theor. Chim. Acta **32**, 111 (1973).
[29] R. Lemke, Synthesis **1974**, 359.
[30] R. Nackaerts, Ph.D. Thesis, University of Leuven, 1983.